THE JOURNAL OF PHYSICAL CHEMISTRY A

Article

pubs.acs.org/JPCA

# $BeCH_2$: The Simplest Metal Carbene. High Levels of Theory

Yudong Qiu, Alexander Yu. Sokolov, Yukio Yamaguchi, and Henry F. Schaefer, III*

Center for Computational Quantum Chemistry, University of Georgia, Athens, Georgia 30602, United States

Supporting Information

**ABSTRACT:** The simplest metal carbene, $BeCH_2$, is experimentally unknown. Its isomer, HBeCH, lies higher in energy, but has been detected by the infrared matrix isolation [*J. Am. Chem. Soc.* **1998**, *120*, 6097]. In the present study the ground and low-lying excited states of the $BeCH_2$ and HBeCH isomers were investigated using state-of-the-art ab initio methods, including coupled-cluster theory with up to full quadruple excitations (CCSDTQ), and complete active space self-consistent field (CASSCF) with multireference configuration interaction with single and double excitations (MRCISD). The relative energies were obtained using the focal point analysis combined with large correlation-consistent cc-pCVXZ basis sets (X = D, T, Q, 5) and were extrapolated to the complete basis set (CBS) limit. The $^3B_1$ state of $BeCH_2$ ($C_{2v}$ symmetry) is the global minimum on the ground triplet potential energy surface (PES). The $^3\Sigma^-$ state of the linear isomer HBeCH is located 4.9 kcal mol$^{-1}$ above the global minimum, at the CCSDTQ/CBS level of theory. The $BeCH_2$ and HBeCH isomers are connected through the $^3A''$ transition state lying 46.1 kcal mol$^{-1}$ above the global minimum. The higher-lying energy HBeCH structure has much larger Be−C bond dissociation energy (126.6 kcal mol$^{-1}$, cf. BDE($BeCH_2$) = 62.1 kcal mol$^{-1}$). The lowest excited state of $BeCH_2$ is the open-shell $^1B_1$ state, with a relative energy of only 4.9 kcal mol$^{-1}$ above the global minimum, followed by $^1A_1$ state (16.8 kcal mol$^{-1}$) at the MRCISD/cc-pCVQZ level of theory. For the HBeCH isomer the lowest-energy excited states are $^1\Delta$ and $^1\Sigma^+$, lying about 30 kcal mol$^{-1}$ above the global minimum. For the ground state of $BeCH_2$ the fundamental vibrational frequencies computed using second-order vibrational perturbation theory (VPT2) at the CCSD(T)/cc-pCVQZ level are reported. We hope that our highly accurate theoretical results will assist in the experimental identification of $BeCH_2$.

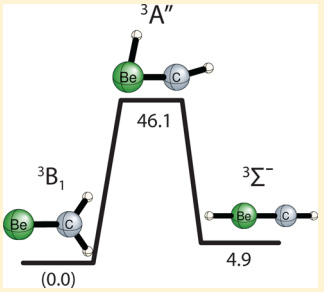


## INTRODUCTION

The development and availability of N-heterocyclic carbenes (NHCs) has resulted in a vast amount of important new chemistry.[1−5] A recent example is the synthesis of the first stable silicon(0) compound with a Si═Si double bond.[6] Yet to be synthesized in a form that might be considered "stable" are the simple metal carbenes Be(NHC), Mg(NHC), and Sr(NHC). Using matrix isolation infrared (IR) spectroscopy, Greene, Lanzisera, Andrews, and Downs[7] have reported HBeCH, a linear isomer of the very simplest metal carbene $BeCH_2$. However, the $C_{2v}$ structure $BeCH_2$ itself remains unknown. Andrews and co-workers have made the parent magnesium compound $MgCH_2$ via matrix isolation.[8] Although the calcium carbene $CaCH_2$ has not yet been made, Orzechowski, Jansen, and Harder have recently synthesized several stable substituted calcium carbenes.[9,10] Although no strontium carbenes have yet been synthesized,[11] there is a report of barium carbenes, again by Orzechowski and Harder.[12]

The present research concerns the very simplest metal carbene $BeCH_2$. It is perhaps unexpected that Greene and co-workers[7] did not identify $BeCH_2$ in their critical matrix isolation study. Early computations suggested that HBeCH, which was unambiguously observed and identified, lies energetically above $BeCH_2$. Luke, Pople and Schleyer[13] noted a substantial barrier between HBeCH and $BeCH_2$. Thus, the nonobservation of $BeCH_2$ may have more to do with the mechanism of the reactions whereby HBeCH was made.

The computational study of $BeCH_2$ isomers began in 1974, when Lamanna and Maestro[14] performed the first unrestricted Hartree−Fock (UHF) studies and found the lowest energy structure to have $C_{2v}$ symmetry with a $^3B_1$ ground state, like the isolated $CH_2$ molecule. Three years later, Schleyer and co-workers[15,16] studied the low-lying triplet and singlet states using second- and third-order Møller−Plesset perturbation theory (MP2 and MP3). In addition to the $^3B_1$ state, they also found a bound $^1A_1$ state lying 29 kcal mol$^{-1}$ higher in energy. Then in 1983, Luke and co-workers[13] extended the electron correlation treatment to MP4. They found a linear HBeCH isomer with a $^3\Sigma^-$ ground state and a $C_s$ symmetry $^3A''$ isomerization transition state, connecting $^3B_1$ $BeCH_2$ and $^3\Sigma^-$ HBeCH. In addition, they used the UHF method in an attempt to describe the open-shell singlet state $^1B_1$. The estimated energy of the $^1B_1$ state was only 5 kcal mol$^{-1}$ higher than the $^3B_1$ global minimum, whereas the relative energy of the $^1A_1$ state was predicted to be 20 kcal mol$^{-1}$. In 2010, Yu and co-workers[17] investigated the reaction pathway of the $^3P$ excited state of Be atom with methane using density function theory (DFT) and quadratic configuration interaction with single and double excitations (QCISD). Among the several pathways found, only the reaction pathway leading to the linear isomer HBeCH was identified.

**Received:** July 3, 2013
**Revised:** August 20, 2013
**Published:** August 23, 2013

Despite the aforementioned work, accurate energetic, structural, and vibrational parameters for the experimentally unknown $BeCH_2$ have not been reported. Here we apply state-of-the-art theoretical methods to $BeCH_2$ to assist in its identification and, hopefully, to inspire organometallic chemists to prepare stable Be(NHC) compounds. We aim to predict the energies, structures, and vibrational frequencies for both ground and low-lying excited states, and elucidate the nature of the chemical bonding in this prototypical compound.

## METHODS

For singlet electronic states, we used the complete active space self-consistent field (CASSCF)[18−20] method with a perturbative treatment of dynamic correlation (CASPT2),[21] and multireference configuration interaction with single and double excitations (MRCISD).[22,23] In the CASSCF computations the active space was chosen to be 12 electrons in 12 orbitals, including core (1s) and valence (2s, 2p) electronic shells of Be and C, and 1s shell of the H atoms. The canonical orbitals were obtained by diagonalizing the effective Fock operator. The MRCISD relative energies were appended with the Davidson correction[24,25] to account for size-consistency; the resulting method was labeled MRCISD+Q. The equilibrium structures were obtained using the MRCISD method with the Dunning's correlation-consistent polarized core−valence cc-pCVQZ[26,27] basis set.

For triplet electronic states, we initially employed the unrestricted Hartree−Fock theory (UHF), second-order Møller−Plesset perturbation theory (MP2), coupled cluster theory incorporating single and double excitations (CCSD)[28−31] and CCSD with perturbative triple excitations [CCSD(T)].[31−33] All electrons were correlated in all computations. To compare the relative energies of triplet and singlet states, we also used the CASSCF, CASPT2, and MRCISD+Q methods. The equilibrium structures on the triplet potential energy surface (PES) were determined at the all-electron CCSD(T) level of theory with the cc-pCVQZ basis set.

The relative energies of the stationary points on the $BeCH_2$ triplet PES were obtained via the focal point analysis technique (FPA),[34,35] using the CCSD(T)/cc-pCVQZ optimized geometries. The complete basis set (CBS) limit values were obtained by extrapolating the Hartree−Fock ($E_{HF}$) and the correlation energies ($E_{corr}$), employing the valence cc-pVXZ (X = D, T, Q, 5) families of basis sets,[26] with the functional forms[36,37]

$$E_{HF}(X) = E_{HF}^{\infty} + ae^{-bX} \quad (1)$$

and

$$E_{corr}(X) = E_{corr}^{\infty} + aX^{-3} \quad (2)$$

respectively. In the FPA computations the 1s orbitals of Be and C were kept frozen. Higher-order correlation effects were accounted for using coupled cluster theory including full single, double, and triple excitations (CCSDT), as well as perturbative and full quadruple excitations [CCSDT(Q) and CCSDTQ].[38] The final energetic results include core correlation corrections $\Delta_{core}$ determined by the difference between all-electron CCSD(T)/cc-pCVQZ and frozen-core CCSD(T)/cc-pVQZ results, zero-point vibrational energy corrections $\Delta_{ZPVE}$ obtained at the all-electron CCSD(T)/cc-pCVQZ level of theory, and diagonal Born−Oppenheimer corrections $\Delta_{DBOC}$ obtained at the all-electron CCSD/cc-pCVQZ level of theory.[39−41]

The harmonic vibrational frequencies were obtained using analytic second derivatives[42,43] of the PES. To account for anharmonicity, we report a second-order vibrational perturbation theory (VPT2)[44] analysis for the $^3B_1$ ground state of $BeCH_2$. The cubic and semidiagonal quartic force constants were obtained by numerical differentiation of the analytic second derivatives with respect to nuclear displacements.

All computations were performed with the CFOUR[45] and MOLPRO[46] software packages. The MRCC program of Kállay[47,48] interfaced with MOLPRO was used to obtain the CCSDT, CCSDT(Q), and CCSDTQ energies.

## RESULTS AND DISCUSSION

**Triplet PES.** *Relative Energies.* The structures of three stationary points on the $BeCH_2$ ground triplet PES are shown in Figure 1. The global minimum on the PES is the $C_{2v}$ symmetry $BeCH_2$ isomer ($^3B_1$ state). Its molecular wave function is well described as a single Slater determinant:

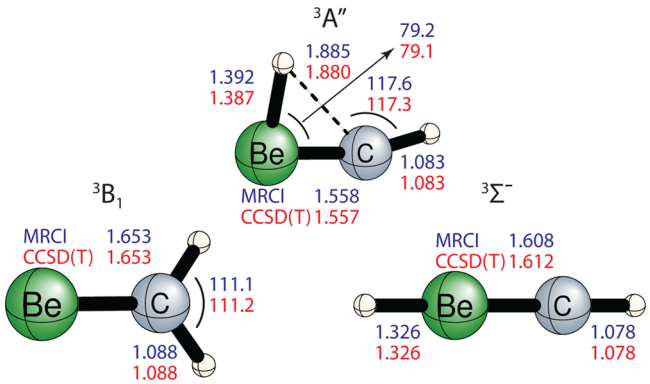


**Figure 1.** Geometries (Å and degrees) of the $^3B_1$ $BeCH_2$ and $^3\Sigma^-$ HBeCH isomers, as well as the $^3A''$ transition state computed using MRCISD and CCSD(T) methods with the core correlated cc-pCVQZ basis set.

$$BeCH_2(^3B_1): \quad [core](4a_1)^2(1b_1\alpha)(5a_1\alpha) \quad (3)$$

where [core] denotes the doubly occupied $(1a_1)^2(2a_1)^2(3a_1)^2(1b_2)^2$ orbitals and $\alpha$ signifies an unpaired electron with spin up. The $^3\Sigma^-$ state of the linear HBeCH isomer ($C_{\infty v}$ symmetry) is the second lowest-energy structure on the triplet PES (Figure 1). Its wave function is represented as:

$$HBeCH(^3\Sigma^-): \quad [core'](5\sigma)^2(1\pi_x\alpha)(1\pi_y\alpha) \quad (4)$$

where $[core'] = (1\sigma)^2(2\sigma)^2(3\sigma)^2(4\sigma)^2$. The valence molecular orbitals of the $BeCH_2$ and HBeCH isomers are shown in Figure 2. The relative energy of the $^3\Sigma^-$ state of the HBeCH isomer was determined using the focal point analysis (Table 1). Taking into account the large zero-point vibrational effects ($\Delta_{ZPVE}$ = −2.2 kcal mol$^{-1}$), as well as the less significant core correlation and diagonal Born−Oppenheimer corrections ($\Delta_{core}$ and $\Delta_{DBOC}$, Table 1), the final value for the relative energy at the CCSDTQ/CBS level of theory was predicted to be 4.9 kcal mol$^{-1}$.

The ground states of the $BeCH_2$ and HBeCH isomers are connected through the $C_s$ symmetry $^3A''$ transition state (Figure 1). Its molecular wave function is described as:


dx.doi.org/10.1021/jp406579w | J. Phys. Chem. A 2013, 117, 9266−9273

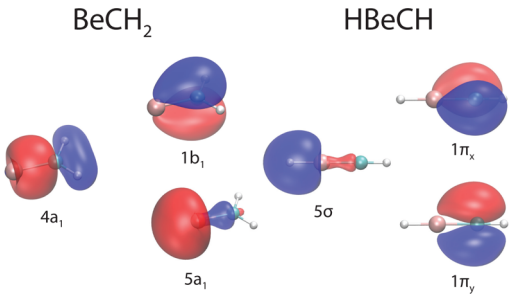


**Figure 2.** Frontier molecular orbitals of the $BeCH_2$ and HBeCH isomers.

$$TS(^3A''): \quad (1a')^2(2a')^2(3a')^2(4a')^2(5a')^2(1a'')^\alpha(1a')^\alpha \tag{5}$$

The focal point analysis for the relative energy of the $^3A''$ transition state (Table 2) exhibits rapid convergence with respect to the electron correlation treatment and the basis set size. Inclusion of quadruple excitations only contributes 0.1 kcal $mol^{-1}$ to the relative energy while the quadruple-$\zeta$ basis set is sufficient to reproduce the extrapolated CBS limit within 0.02 kcal $mol^{-1}$ accuracy. Including $\Delta_{core}$, $\Delta_{ZPVE}$, and $\Delta_{DBOC}$ corrections, we obtain the 46.1 kcal $mol^{-1}$ value for the energy of $^3A''$ transition state relative to $^3B_1$ $BeCH_2$ at the CCSDTQ/CBS level of theory.

The relative energies of the stationary points on the triplet $BeCH_2$ PES are summarized in Figure 3. The large relative energy of the $^3A''$ transition state guarantees a substantial barrier on the PES. In particular, the activation energy for the isomerization from HBeCH to $BeCH_2$ amounts to 41.2 kcal $mol^{-1}$ at the CCSDTQ/CBS level of theory.

*Structures and Molecular Orbital Analysis.* The optimized structures of the three stationary points on the triplet PES computed using CCSD(T) and MRCISD methods with the cc-pCVQZ basis set are shown in Figure 1. The geometric parameters obtained using the two methods are the same to 0.005 Å and 0.3°. Thus, only the CCSD(T) geometries will be discussed hereafter. The global minimum structure has the longest Be−C bond length (1.653 Å), of the three geometries shown in Figure 1. The Be−C distances of the $^3\Sigma^-$ HBeCH isomer and $^3A''$ transition state are 1.612 Å and 1.557 Å, respectively. Computed Wiberg bond indices[49] (0.31 and 0.41 for $BeCH_2$ and HBeCH, respectively) indicate a stronger Be−C bonding interaction in HBeCH, compared to $BeCH_2$. Interestingly, coordination of the Be atom to the $CH_2$ radical results in the significant reduction of the ∠HCH bond angle from 132° in the ground $^3B_1$ state of $CH_2$[50] to 111° in the $^3B_1$ $BeCH_2$.

Figure 4 shows a simplified diagram correlating the $^3B_1$ $BeCH_2$ frontier molecular orbitals (MOs) to the MOs of the ground state $^1S_g$ Be and $^3B_1$ $CH_2$ fragments. Interaction of the Be 2s and $2p_z$ orbitals with the $3a_1$ $CH_2$ MO gives rise to two frontier $\sigma$-type MOs ($4a_1$ and $5a_1$). Among them, the $4a_1$ MO is mostly localized on the $CH_2$ fragment and describes weak $\sigma$-bonding, while $5a_1$ is largely a nonbonding MO, composed of 2s and $2p_z$ orbitals of Be (Figures 2 and 4). The $\sigma$-type interaction between Be and $CH_2$ can be characterized as a weak donation of the electron density from the filled 2s Be orbital to the half-filled $3a_1$ orbital of $CH_2$ radical. The increase of the $CH_2$ $3a_1$ fragment orbital occupation, which favors the bending of the $CH_2$ moiety,[51] may explain the reduction of ∠HCH bond angle in $BeCH_2$, mentioned above. Mixing of the out-of-plane Be $2p_x$ orbital with the $1b_1$ $CH_2$ MO results in the two $\pi$-type $1b_1$ and $2b_1$ $BeCH_2$ MOs, of bonding and antibonding character, respectively. The $1b_1$ MO describes a weak $\pi$-donation from $CH_2$ $\pi$-type orbital, perpendicular to the plane of the molecule, to the unoccupied p-orbital of Be. Overall, our analysis indicates that the orbital interaction of the Be and $CH_2$ fragments is rather weak and is consistent with the small value of the computed Wiberg Be−C bond index and relatively long bond distance.

*Vibrational Frequencies.* The theoretically predicted harmonic and fundamental vibrational frequencies and associated infrared (IR) intensities for the ground $^3B_1$ state of $BeCH_2$ are presented in Table 3. The two most intense vibrational modes, $\nu_3$ and $\nu_4$, correspond to Be−C stretching and $CH_2$ wagging, respectively. The $\nu_1$, $\nu_5$, and $\nu_6$ modes are predicted to have low IR intensities, which may make their spectroscopic identification difficult.

The fundamental vibrational frequencies were determined using the VPT2 theory. In the anharmonic analysis the $\nu_2$ mode suffered from a Fermi type I resonances ($2\nu_4 \approx \nu_2$). The effect of the resonance was estimated by computing the eigenvalues of the vibrational configuration interaction matrix:

$$\begin{pmatrix} \omega_2 & \phi_{2-2-4}/\sqrt{2} \\ \phi_{2-2-4}/\sqrt{2} & 2\omega_4 \end{pmatrix} \tag{6}$$

**Table 1. Focal Point Analysis of the Linear HBeCH Isomer $^3\Sigma^-$ Ground State Energy Relative to the $^3B_1$ $BeCH_2$ Global Minimum ($\Delta E$, kcal $mol^{-1}$)[a]**

| basis set | $\Delta E$[UHF] | $\delta$[MP2] | $\delta$[CCSD] | $\delta$[CCSD(T)] | $\delta$[CCSDT] | $\delta$[CCSDT(Q)] | $\delta$[CCSDTQ] | $\Delta E$[CCSDTQ] |
|---|---|---|---|---|---|---|---|---|
| cc-pVDZ | +2.79 | +4.63 | −3.32 | +0.62 | −0.02 | +0.04 | −0.01 | [+4.74] |
| cc-pVTZ | +3.49 | +5.45 | −3.34 | +0.87 | −0.06 | +0.05 | −0.00 | [+6.45] |
| cc-pVQZ | +3.40 | +5.73 | −3.20 | +0.92 | −0.07 | [+0.05] | [−0.00] | [+6.82] |
| cc-pV5Z | +3.43 | +5.81 | −3.15 | +0.94 | [−0.07] | [+0.05] | [−0.00] | [+7.01] |
| CBS limit | [+3.46] | [+5.90] | [−3.09] | [+0.96] | [−0.07] | [+0.05] | [−0.00] | [**+7.20**] |
| $\Delta E$ (final) = $\Delta E$[CCSDTQ/CBS] + $\Delta_{ZPVE}$[CCSD(T)/cc-pCVQZ] + $\Delta_{core}$[CCSD(T)/cc-pCVQZ] + $\Delta_{DBOC}$[CCSD/cc-pCVQZ] = 7.20 − 2.20 − 0.17 + 0.02 = **4.85** kcal $mol^{-1}$ | | | | | | | | |
| fit function | $a+be^{-cX}$ | $a+bX^{-3}$ | $a+bX^{-3}$ | $a+bX^{-3}$ | additive | additive | additive | |
| points ($X$) | 3,4,5 | 4,5 | 4,5 | 4,5 | | | | |

[a]The symbol $\delta$ denotes the increment in the relative energy with respect to the preceding level of theory in the hierarchy UHF→MP2→CCSD→CCSD(T)→CCSDT→CCSDT(Q)→CCSDTQ. Square brackets signify results obtained from basis set extrapolations or additivity assumptions. Final predictions are boldfaced.


dx.doi.org/10.1021/jp406579w | J. Phys. Chem. A 2013, 117, 9266−9273

**Table 2. Focal Point Analysis of the $^3A''$ Transition State Energy Relative to the $^3B_1$ $BeCH_2$ Global Minimum ($\Delta E$, kcal mol$^{-1}$)[a]**

| basis set | $\Delta E$[UHF] | $\delta$[MP2] | $\delta$[CCSD] | $\delta$[CCSD(T)] | $\delta$[CCSDT] | $\delta$[CCSDT(Q)] | $\delta$[CCSDTQ] | $\Delta E$[CCSDTQ] |
|---|---|---|---|---|---|---|---|---|
| cc-pVDZ | +62.86 | −6.15 | −5.72 | −1.43 | −0.32 | −0.10 | −0.00 | [+49.13] |
| cc-pVTZ | +63.17 | −6.03 | −5.54 | −1.53 | −0.32 | −0.15 | +0.00 | [+49.61] |
| cc-pVQZ | +63.01 | −6.01 | −5.43 | −1.60 | −0.30 | [−0.15] | [+0.00] | [+49.51] |
| cc-pV5Z | +63.03 | −6.04 | −5.40 | −1.62 | [−0.30] | [−0.15] | [+0.00] | [+49.52] |
| CBS limit | [+63.05] | [−6.07] | [−5.36] | [−1.65] | [−0.30] | [−0.15] | [+0.00] | **[+49.53]** |
| $\Delta E$ (final) = $\Delta E$[CCSDTQ/CBS] + $\Delta_{ZPVE}$[CCSD(T)/cc-pCVQZ] + $\Delta_{core}$[CCSD(T)/cc-pCVQZ] + $\Delta_{DBOC}$[CCSD/cc-pCVQZ] = 49.53 − 3.46 − 0.08 + 0.08 = **46.06 kcal mol$^{-1}$** | | | | | | | | |
| fit function | $a+be^{-cX}$ | $a+bX^{-3}$ | $a+bX^{-3}$ | $a+bX^{-3}$ | additive | additive | | |
| points ($X$) | 3,4,5 | 4,5 | 4,5 | 4,5 | | | | |

[a]The symbol $\delta$ denotes the increment in the relative energy with respect to the preceding level of theory in the hierarchy UHF→MP2→CCSD→CCSD(T)→CCSDT→CCSDT(Q)→CCSDTQ. Square brackets signify results obtained from basis set extrapolations or additivity assumptions. Final predictions are boldfaced.

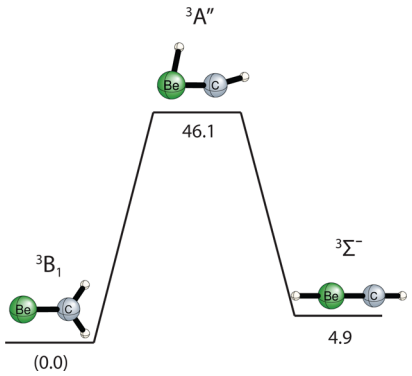


**Figure 3.** Schematic representation of the $BeCH_2$ triplet PES. Relative energies (kcal mol$^{-1}$) are computed at the CCSDTQ/CBS level of theory using focal point analysis.

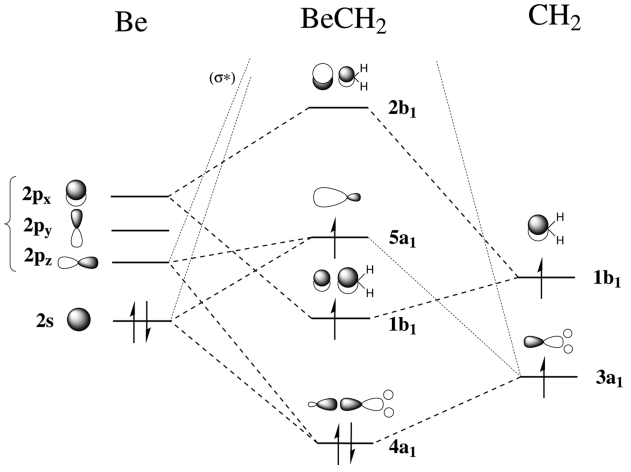


**Figure 4.** Simplified correlation diagram for the formation of $^3B_1$ $BeCH_2$ from $^1S$ Be and $^3B_1$ $CH_2$ fragments. Only the four $BeCH_2$ orbitals are shown for simplicity. The curly brace on the left indicates the degeneracy of Be p-orbitals. Large contributions of fragment orbitals are indicated by the dashed lines, while small contributions are depicted by the dotted lines.

The off-diagonal elements are the cubic force constants ($\phi_{2-2-4}$ = 211.7 cm$^{-1}$). Fermi resonance shifts the $\nu_2$ mode by 136 cm$^{-1}$, giving rise to the final fundamental value of 1490 cm$^{-1}$.

The harmonic frequencies and IR intensities for the $^3\Sigma^-$ state of HBeCH are reported in Table 4. The theoretically predicted harmonic vibrational frequencies of the high intensity modes ($\omega_2$ = 2175 cm$^{-1}$, $\omega_3$ = 1016 cm$^{-1}$, $\omega_4$ = 536 cm$^{-1}$) are in a good agreement with the fundamental frequencies obtained from infrared matrix isolation experiment ($\omega_2$ = 2114 cm$^{-1}$, $\omega_3$ = 998 cm$^{-1}$, $\omega_4$ = 526 cm$^{-1}$).[7] The remaining $\omega_1$ and $\omega_5$ modes were predicted to have low intensities, and were not observed in the experiment. The harmonic frequencies and IR intensities for the $^3A''$ transition state are shown in Supporting Information, Table S2. The $\omega_3$ reaction coordinate mode exhibits the large imaginary frequency of 1315$i$ cm$^{-1}$.

**Table 3. Harmonic and Fundamental Vibrational Frequencies (cm$^{-1}$), as well as the Corresponding Infrared Intensities[a] of the $BeCH_2$ $^3B_1$ Global Minimum Computed at the CCSD(T)/cc-pCVQZ Level of Theory**

| symmetry | modes | harmonic | fundamental | assignment |
|---|---|---|---|---|
| $a_1$ | $\nu_1$ | 3096 (3.6) | 2965 | $CH_2$ symmetric stretching |
| | $\nu_2$ | 1395 (10.9) | 1490 | $CH_2$ scissoring |
| | $\nu_3$ | 957 (55.1) | 937 | Be−C stretching |
| $b_1$ | $\nu_4$ | 683 (46.7) | 674 | $CH_2$ wagging |
| $b_2$ | $\nu_5$ | 3174 (3.2) | 3025 | $CH_2$ antisymmetric stretching |
| | $\nu_6$ | 539 (0.0) | 523 | $CH_2$ rocking |

[a]In parentheses, km mol$^{-1}$.

**Table 4. Harmonic Vibrational Frequencies[a] and Infrared Intensities[b] of the $^3\Sigma^-$ State of HBeCH Computed at the CCSD(T)/cc-pCVQZ Level of Theory**

| symmetry | mode | $\omega_e$ | IR intensity |
|---|---|---|---|
| $\Sigma^+$ | $\omega_1$ | 3258 | 3 |
| | $\omega_2$ | 2175 | 179 |
| | $\omega_3$ | 1016 | 69 |
| $\Pi$ | $\omega_4$ | 536 | 192 |
| | $\omega_5$ | 393 | 13 |

[a]$\omega_e$ in km mol$^{-1}$. [b]In cm$^{-1}$.

*Bond Dissociation Energy.* One of the most important characteristics of the stability of metal-carbene complexes is the bond dissociation energy (BDE). The BDE of the ground $^3B_1$ state of $BeCH_2$ was obtained using the focal point analysis, according to the following equations:

$$BeCH_2(^3B_1) \rightarrow Be(^1S) + CH_2(^3B_1) \quad (7)$$

$$BDE = E_{Be} + E_{CH_2} - E_{BeCH_2} \quad (8)$$

Table 5 shows the effect of the electron correlation treatment on the computed BDE values. At the UHF/CBS level of theory, the BDE was computed to be 57.0 kcal mol$^{-1}$. Perturbative


dx.doi.org/10.1021/jp406579w | J. Phys. Chem. A 2013, 117, 9266−9273

Table 5. Focal Point Analysis of the $BeCH_2$ Global Minimum ($^3B_1$ State) Be−C Bond Dissociation Energy (BDE, kcal mol$^{-1}$)[a]

| basis set | BDE[UHF] | δ[MP2] | δ[CCSD] | δ[CCSD(T)] | δ[CCSDT] | δ[CCSDT(Q)] | δ[CCSDTQ] | BDE[CCSDTQ] |
|---|---|---|---|---|---|---|---|---|
| cc-pVDZ | +55.64 | +9.79 | −10.38 | +1.38 | +0.17 | +0.09 | −0.00 | [+56.69] |
| cc-pVTZ | +56.59 | +12.94 | −10.01 | +1.95 | +0.10 | +0.10 | +0.00 | [+61.68] |
| cc-pVQZ | +56.98 | +14.21 | −9.96 | +2.09 | +0.08 | [+0.10] | [+0.00] | [+63.50] |
| cc-pV5Z | +57.00 | +14.68 | −10.01 | +2.13 | [+0.08] | [+0.10] | [+0.00] | [+63.98] |
| CBS limit | [+56.98] | [+15.17] | [−10.06] | [+2.18] | [+0.08] | [+0.10] | [+0.00] | **[+64.45]** |
| BDE (final) = BDE[CCSDTQ/CBS] + $\Delta_{ZPVE}$[CCSD(T)/cc-pCVQZ] + $\Delta_{core}$[CCSD(T)/cc-pCVQZ] + $\Delta_{DBOC}$[CCSD/cc-pCVQZ] = 64.45 − 3.17 + 0.86 − 0.01 = **62.13 kcal mol$^{-1}$** | | | | | | | | |
| fit function | $a+be^{-cX}$ | $a+bX^{-3}$ | $a+bX^{-3}$ | $a+bX^{-3}$ | additive | additive | additive | |
| points ($X$) | 3,4,5 | 4,5 | 4,5 | 4,5 | | | | |

[a]The symbol δ denotes the increment in the bond dissociation energy (BDE) with respect to the preceding level of theory in the hierarchy UHF→MP2→CCSD→CCSD(T)→CCSDT→CCSDT(Q)→CCSDTQ. Square brackets signify results obtained from basis set extrapolations or additivity assumptions. Final predictions are boldfaced.

Table 6. Focal Point Analysis of the Linear HBeCH Isomer ($^3\Sigma^-$ State) Be−C Bond Dissociation Energy (BDE, kcal mol$^{-1}$)[a]

| basis set | BDE[UHF] | δ[MP2] | δ[CCSD] | δ[CCSD(T)] | δ[CCSDT] | δ[CCSDT(Q)] | δ[CCSDTQ] | BDE[CCSDTQ] |
|---|---|---|---|---|---|---|---|---|
| cc-pVDZ | +93.53 | +25.87 | +0.99 | +0.95 | +0.10 | +0.07 | +0.00 | [+121.52] |
| cc-pVTZ | +94.29 | +31.42 | +0.15 | +1.48 | +0.04 | +0.08 | +0.01 | [+127.46 |
| cc-pVQZ | +94.41 | +33.58 | −0.47 | +1.61 | +0.01 | [+0.08] | [+0.01] | [+129.23] |
| cc-pV5Z | +94.40 | +34.44 | −0.84 | +1.65 | [+0.01] | [+0.08] | [+0.01] | [+129.74] |
| CBS limit | [+94.39] | [+35.34] | [−1.24] | [+1.69] | [+0.01] | [+0.08] | [+0.01] | **[+130.27]** |
| BDE (final) = BDE[CCSDTQ/CBS] + $\Delta_{ZPVE}$[CCSD(T)/cc-pCVQZ] + $\Delta_{core}$[CCSD(T)/cc-pCVQZ] + $\Delta_{DBOC}$[CCSD/cc-pCVQZ] = 130.27 − 4.46 + 0.82 + 0.01 = **126.64 kcal mol$^{-1}$** | | | | | | | | |
| fit function | $a+be^{-cX}$ | $a+bX^{-3}$ | $a+bX^{-3}$ | $a+bX^{-3}$ | additive | additive | additive | |
| points ($X$) | 3,4,5 | 4,5 | 4,5 | 4,5 | | | | |

[a]The symbol δ denotes the increment in the bond dissociation energy (BDE) with respect to the preceding level of theory in the hierarchy UHF→MP2→CCSD→CCSD(T)→CCSDT→CCSDT(Q)→CCSDTQ. Square brackets signify results obtained from basis set extrapolations or additivity assumptions. Final predictions are boldfaced.

Table 7. Energies of $BeCH_2$ and HBeCH Isomers, as well as $^3A''$ Transition State Relative to the $^3B_1$ $BeCH_2$ Global Minimum at Five Different Levels of Theory with the cc-pCVQZ Basis Set (kcal mol$^{-1}$)

| isomer | state | E(CASSCF) | E(CASPT2) | E(MRCISD+Q) | E(CCSD) | E(CCSD(T)) |
|---|---|---|---|---|---|---|
| $BeCH_2$ | $^3B_1$ | 0.0 | 0.0 | 0.0 | 0.0 | 0.0 |
| $BeCH_2$ | $^1B_1$ | 5.0 | 4.6 | 4.9 | | |
| $BeCH_2$ | $^1A_1$ | 20.8 | 18.5 | 16.8 | | |
| HBeCH | $^3\Sigma^-$ | 21.3 | 5.4 | 7.3 | 5.8 | 6.7 |
| HBeCH | $^1\Delta$ | 37.9 | 30.4 | 30.0 | | |
| HBeCH | $^1\Sigma^+$ | 51.0 | 30.6 | 30.0 | | |
| TS | $^3A''$ | 53.4 | 50.2 | 49.7 | 51.2 | 49.9 |

inclusion of the double excitations at the MP2 level results in a large positive correction (δ[MP2] = +15.2 kcal mol$^{-1}$). Including full double excitations at the CCSD level (δ[CCSD] = −10.1 kcal mol$^{-1}$) lowers the value of BDE substantially. The perturbative triple excitations still provide an important contribution (+2.2 kcal mol$^{-1}$). The effect of the higher-order corrections is not negligible. Taking the zero-point vibrational energy into account ($\Delta_{ZPVE}$ = −3.2 kcal mol$^{-1}$), and adding the $\Delta_{core}$ and $\Delta_{DBOC}$ corrections (+0.9 and −0.01 kcal mol$^{-1}$, respectively), the final BDE is predicted to be 62.1 kcal mol$^{-1}$.

For the $^3\Sigma^-$ HBeCH isomer the BDE was computed as follows:

$$HBeCH(^3\Sigma^-) \rightarrow HBe(^2\Sigma^+) + CH(^4\Sigma^-) \quad (9)$$

$$BDE = E_{HBe} + E_{CH} - E_{HBeCH} \quad (10)$$

The focal point analysis for the BDE in eqs 9 and 10 is shown in Table 6. The $^3\Sigma^-$ HBeCH BDE value (126.6 kcal mol$^{-1}$) computed at the CCSDTQ/CBS level of theory is larger than that of global minimum $^3B_1$ $BeCH_2$ isomer (62.1 kcal mol$^{-1}$) by more than a factor of 2. Thus, the lower energy of $^3B_1$ $BeCH_2$, compared to $^3\Sigma^-$ HBeCH, is a result of the energetic preference for the formation of two C−H bonds in contrast to one C−H and one Be−H bond. The larger BDE value in $^3\Sigma^-$ HBeCH is in agreement with the shorter Be−C bond length and larger Wiberg bond order than those for $^3B_1$ $BeCH_2$.

**Singlet Excited States.** *Relative Energies.* The relative energies of several stationary points on the triplet and singlet PESs computed using five different methods with the cc-pCVQZ basis set are shown in Table 7. For the triplet states the energies obtained at the MRCISD+Q and CCSD(T) levels of theory differ by at most 0.6 kcal mol$^{-1}$ only. At the MRCISD +Q/cc-pCVQZ level of theory the lowest-energy excited state of $BeCH_2$ isomer is the open-shell $^1B_1$ state, lying adiabatically 4.9 kcal mol$^{-1}$ above the global minimum. The $^1B_1$ electronic wave function can be represented as

$$BeCH_2(^1B_1): \quad [core](4a_1)^2[(1b_1\alpha)(5a_1\beta) - (1b_1\beta)(5a_1\alpha)] \quad (11)$$


dx.doi.org/10.1021/jp406579w | J. Phys. Chem. A 2013, 117, 9266−9273

which is an antisymmetric combination of two equally important determinants. Interestingly, at the same level of theory without the zero-point vibrational correction, the $^1B_1$ $BeCH_2$ excited state is lying lower in energy than the experimentally observed $^3\Sigma^-$ ground state of HBeCH (7.3 kcal mol$^{-1}$ above the global minimum, Table 7).

The $^1B_1$ excited state of $BeCH_2$ is followed in energy by the $^1A_1$ state, which has the following dominant electronic configuration:

$$BeCH_2(^1A_1): \quad [core](4a_1)^2(1b_1)^2 \tag{12}$$

The energy of the $^1A_1$ $BeCH_2$ excited state is 16.8 kcal mol$^{-1}$ relative to the global minimum $^3B_1$ $BeCH_2$ at the MRCISD+Q/cc-pCVQZ level of theory, which gives rise to a 11.9 kcal mol$^{-1}$ energy separation between the two singlet states of $BeCH_2$.

For the linear HBeCH isomer the two lowest excited states are $^1\Delta$ and $^1\Sigma^+$. Both of these states have a two-determinant molecular wave function arising from $(1\pi)^2$ electronic configuration:

$$HBeCH(^1\Delta^+): [core'][(1\pi_x)^2 - (1\pi_y)^2]$$

$$HBeCH(^1\Delta^-): [core'][(1\pi_x\alpha)(1\pi_y\beta) - (1\pi_x\beta)(1\pi_y\alpha)] \tag{13}$$

$$HBeCH(^1\Sigma^+): \quad [core'][(1\pi_x)^2 + (1\pi_y)^2] \tag{14}$$

While at the CASSCF/cc-pCVQZ level of theory the energy levels of these two states are separated by 13.1 kcal mol$^{-1}$, perturbative treatment of the dynamic correlation at the CASPT2/cc-pCVQZ level reduces the energy difference to 0.2 kcal mol$^{-1}$ (Table 7). At the MRCISD+Q level of theory the energy difference becomes even smaller (0.02 kcal mol$^{-1}$), indicating that the two states are almost degenerate with adiabatic excitation energies about 30 kcal mol$^{-1}$ above the $BeCH_2$ global minimum.

*Structures and Bonding Analysis.* The equilibrium geometries of the $BeCH_2$ and HBeCH singlet states computed at the MRCISD/cc-pCVQZ level of theory are shown in Figure 5.

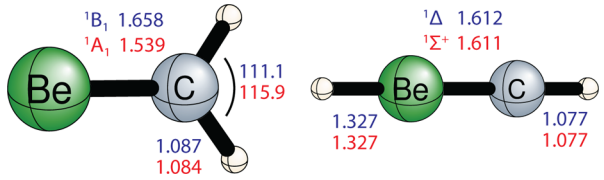


**Figure 5.** Geometries (Å and degrees) of the lowest-energy singlet states of $BeCH_2$ and HBeCH isomers optimized at the MRCISD/cc-pCVQZ level of theory.

The geometrical parameters of the $^1B_1$ state of $BeCH_2$ are very close to those of the $^3B_1$ ground state (Figure 1). On the other hand, the $^1A_1$ excited state has a significantly shorter Be−C bond length and a larger ∠HCH bond angle than the $^3B_1$ and $^1B_1$ states of $BeCH_2$, and also has a larger Wiberg index (1.15). For the linear geometries, the $^1\Delta$ and $^1\Sigma^+$ states have almost identical geometries, which are very similar to that of the $^3\Sigma^-$ state.

The large structural differences of the $^1A_1$ excited $BeCH_2$ state compared to the global minimum structure can be rationalized from an analysis of the correlation diagram in Figure 4. In the $^1A_1$ state the $5a_1$ MO is left vacant, while the $\pi$-type bonding $1b_1$ MO is doubly occupied, which leads to the predicted shortening of the Be−C distance. Compression of the Be−C bond may result in the less efficient $\sigma$-bonding, described by the $4a_1$ MO, and smaller contribution of the $CH_2$ orbitals. The latter may explain the increase of the ∠HCH bond angle by about 5°.

## CONCLUSIONS

In the present research, the ground and excited states of the simplest metal carbene, $BeCH_2$, and its HBeCH isomer have been theoretically studied using high-level ab initio methods. On the triplet PES three stationary points were investigated and their geometric parameters were optimized at the CCSD(T)/cc-pCVQZ level of theory. The global minimum was found to be $^3B_1$ state of $BeCH_2$ isomer ($C_{2v}$ symmetry). Using a highly accurate focal point analysis (FPA) methodology we determined the relative energy of the HBeCH isomer ($^3\Sigma^-$ ground state) to be 4.9 kcal mol$^{-1}$ at the CCSDTQ/CBS level of theory, including zero-point vibrational, core correlation, and diagonal Born−Oppenheimer corrections. By characterizing the transition state connecting $BeCH_2$ and HBeCH isomers the reaction barrier for this endothermic isomerization was determined to be 46.1 kcal mol$^{-1}$.

To investigate the thermodynamic viability of the $BeCH_2$ and HBeCH isomers with respect to the Be−C bond breaking we computed the Be−C bond dissociation energies (BDEs) using the FPA. Despite lying higher in energy, the BDE for the linear HBeCH is more than two times larger than that of $BeCH_2$. In addition to high-level harmonic vibrational constants for all triplet stationary points, for the experimentally unknown $BeCH_2$ isomer we reported the fundamental vibrational frequencies computed at the CCSD(T)/cc-pCVQZ level of theory. The theoretical analysis of low-lying singlet excited states of $BeCH_2$ ($^1B_1$ and $^1A_1$) and HBeCH ($^1\Delta$ and $^1\Sigma^+$) isomers requires the treatment of multideterminant reference wave functions. At the MRCISD+Q/cc-pCVQZ level of theory the relative energies (in kcal mol$^{-1}$) of all triplet and singlet stationary points were found to be as follows: $^3B_1$ (0.0) < $^1B_1$ (4.9) < $^3\Sigma^-$ (7.3) < $^1A_1$ (16.8) < $^1\Delta$ (30.0) ≈ $^1\Sigma^+$ (30.0) < $^3A''$ (49.7).

One of the puzzling questions about the $BeCH_2$ molecule is why the $^3B_1$ ground state has not yet been detected experimentally. Earlier studies, as well as the results of the present work, evidence that $BeCH_2$ exhibits all properties of a thermodynamical viable molecule. It is therefore possible that the nonobservation of $BeCH_2$ in experiments[7] has something to do with its kinetic persistence or the mechanism of the reaction used for the synthesis. We conclude that the latter factor is likely the reason. Taking into account the large energy barrier between the two isomers, it appears that reaction conditions that involve the generation of the $CH_2$ in the gas phase may favor the formation of $BeCH_2$ more than the established reaction of Be with methane.[7] In the latter case the possibility for the Be insertion into C−H bond is more likely and, thus, only HBeCH can be produced. Overall, we hope that the theoretically predicted properties reported herein will be used to assist the future experimental characterization of $BeCH_2$.

## ASSOCIATED CONTENT

### Supporting Information

Tables containing theoretically predicted harmonic vibrational frequencies for the $^3\Sigma^-$ state of HBeCH isomer, $^3A''$ transition


dx.doi.org/10.1021/jp406579w | J. Phys. Chem. A 2013, 117, 9266−9273

state, as well as singlet excited states. This material is available free of charge via the Internet at http://pubs.acs.org.

## AUTHOR INFORMATION


### Corresponding Author

*E-mail: qc@uga.edu.


### Notes

The authors declare no competing financial interest.

## ACKNOWLEDGMENTS

This work was supported by the U.S. Department of Energy, Office of Basic Energy Sciences, Combustion Program (Grant DEFG02-97-ER14748). Y.Q. thanks Dr. Jay Agarwal for the help with the anharmonic analysis using vibrational perturbation theory.

## REFERENCES


(1) Arduengo, A. J.; Harlow, R. L.; Kline, M. A stable crystalline carbene. *J. Am. Chem. Soc.* **1991**, *113*, 361−363.

(2) Arduengo, A. J. Looking for stable carbenes: the difficulty in starting anew. *Acc. Chem. Res.* **1999**, *32*, 913−921.

(3) Bourissou, D.; Guerret, O.; Gabba, F. P.; Bertrand, G. Stable Carbenes. *Chem. Rev.* **2000**, *100*, 39−92.

(4) Trnka, T. M.; Grubbs, R. H. The development of $L_2X_2Ru$ = CHR olefin metathesis catalysts: an organometallic success story. *Acc. Chem. Res.* **2001**, *34*, 18−29.

(5) Herrmann, W. A. N-Heterocyclic Carbenes: A New Concept in Organometallic Catalysis. *Angew. Chem., Int. Ed.* **2002**, *41*, 1290−1309.

(6) Wang, Y.; Xie, Y.; Wei, P.; King, R. B.; Schaefer, H. F.; von R. Schleyer, P.; Robinson, G. H. A stable silicon(0) compound with a Si=Si double bond. *Science* **2008**, *321*, 1069−1071.

(7) Greene, T. M.; Lanzisera, D. V.; Andrews, L.; Downs, A. J. A Matrix-Isolation and Density Functional Theory Study of the Reactions of Laser-Ablated Beryllium, Magnesium, and Calcium Atoms with Methane. *J. Am. Chem. Soc.* **1998**, *120*, 6097−6104.

(8) William, D.; Citra, A.; Trindle, C.; Andrews, L. Matrix infrared spectroscopic study of magnesium carbene and carbenoid radicals and analysis of their bonding with density functional calculations. *Inorg. Chem.* **2000**, *39*, 1204−1215.

(9) Orzechowski, L.; Jansen, G.; Harder, S. Synthesis, structure, and reactivity of a stabilized calcium carbene: $R_2CCa$. *J. Am. Chem. Soc.* **2006**, *128*, 14676−14684.

(10) Orzechowski, L.; Harder, S. Isolation of an Intermediate in the Catalytic Trimerization of Isocyanates by a Monomeric Calcium Carbene with Chelating Iminophosphorane Substituents. *Organometallics* **2007**, *26*, 2144−2148.

(11) Liddle, S. T.; Mills, D. P.; Wooles, A. J. Early metal bis(phosphorus-stabilised)carbene chemistry. *Chem. Soc. Rev.* **2011**, *40*, 2164−2176.

(12) Orzechowski, L.; Harder, S. Syntheses, Structures, and Reactivity of Barium Carbene Complexes with Chelating Bis-iminophosphorano Arms. *Organometallics* **2007**, *26*, 5501−5506.

(13) Luke, B. T.; Pople, J. A.; von Ragué Schleyer, P. A theoretical comparison of the lowest-lying singlet and triplet states of $H_2CBe$ and of HCBeH. *Chem. Phys. Lett.* **1983**, *97*, 265−269.

(14) Lamanna, U.; Maestro, M. Ab initio calculations for ground states of $CH_2Li^-$ and $CH_2Be$. *Theor. Chim. Acta* **1974**, *36*, 103−108.

(15) Binkley, J. S.; Seeger, R.; Pople, J. A.; Dill, J. D.; Schleyer, P. R. Carbon-beryllium binding in $CH_2Be$. *Theor. Chim. Acta.* **1977**, *45*, 69−72.

(16) Dill, J. D.; Schleyer, P. R.; Binkley, J. S.; Pople, J. A. Molecular orbital theory of the electronic structure of molecules. 34. Structures and energies of small compounds containing lithium or beryllium. Ionic, multicenter, and coordinate bonding. *J. Am. Chem. Soc.* **1977**, *99*, 6159−6173.

(17) Yu, Y.; Yu, F.; Zhou, X. Theoretical study on the reaction of $Be(^3P)$ with methane. *J. Mol. Struct.* **2010**, *942*, 66−70.

(18) Werner, H.-J.; Knowles, P. J. A second order multiconfiguration SCF procedure with optimum convergence. *J. Chem. Phys.* **1985**, *82*, 5053−5063.

(19) Knowles, P. J.; Werner, H. J. An efficient second-order MC SCF method for long configuration expansions. *Chem. Phys. Lett.* **1985**, *115*, 259−267.

(20) Roos, B. O. In *Advances in Chemical Physics*; Lawley, K. P., Ed.; Advances in Chemical Physics; John Wiley & Sons, Inc.: Hoboken, NJ, 1987; Vol. *69*.

(21) Andersson, K.; Malmqvist, P. A.; Roos, B. O.; Sadlej, A. J.; Wolinski, K. Second-order perturbation theory with a CASSCF reference function. *J. Phys. Chem.* **1990**, *94*, 5483−5488.

(22) Werner, H.-J.; Knowles, P. J. An efficient internally contracted multiconfiguration−reference configuration interaction method. *J. Chem. Phys.* **1988**, *89*, 5803−5814.

(23) Knowles, P. J.; Werner, H. J. An efficient method for the evaluation of coupling coefficients in configuration interaction calculations. *Chem. Phys. Lett.* **1988**, *145*, 514−522.

(24) Langhoff, S. R.; Davidson, E. R. Configuration interaction calculations on the nitrogen molecule. *Int. J. Quantum Chem.* **1974**, *8*, 61−72.

(25) Meissner, L. Size-consistency corrections for configuration interaction calculations. *Chem. Phys. Lett.* **1988**, *146*, 204−210.

(26) Dunning, T. H. Gaussian basis sets for use in correlated molecular calculations. I. The atoms boron through neon and hydrogen. *J. Chem. Phys.* **1989**, *90*, 1007−1023.

(27) Woon, D. E.; Dunning, T. H. Gaussian basis sets for use in correlated molecular calculations. III. The atoms aluminum through argon. *J. Chem. Phys.* **1993**, *98*, 1358−1371.

(28) Rittby, M.; Bartlett, R. J. An open-shell spin-restricted coupled cluster method: application to ionization potentials in nitrogen. *J. Phys. Chem.* **1988**, *92*, 3033−3036.

(29) Stanton, J. F.; Gauss, J.; Watts, J. D.; Bartlett, R. J. A Direct Product Decomposition Approach for Symmetry Exploitation in Many-Body Methods. I. Energy Calculations. *J. Chem. Phys.* **1991**, *94*, 4334−4345.

(30) Hampel, C.; Peterson, K. A.; Werner, H.-J. A Comparison of the Efficiency and Accuracy of the Quadratic Configuration Interaction (QCISD), Coupled Cluster (CCSD), and Brueckner Coupled Cluster (BCCD) Methods. *Chem. Phys. Lett.* **1992**, *190*, 1−12.

(31) Watts, J. D.; Gauss, J.; Bartlett, R. J. Open-shell analytical energy gradients for triple excitation many-body, coupled-cluster methods: MBPT(4), CCSD+T(CCSD), CCSD(T),and QCISD(T). *Chem. Phys. Lett.* **1992**, *200*, 1−7.

(32) Raghavachari, K.; Trucks, G. W.; Pople, J. A.; Head-Gordon, M. A fifth-order perturbation comparison of electron correlation theories. *Chem. Phys. Lett.* **1989**, *157*, 479−483.

(33) Stanton, J. F. Why CCSD(T) works: a different perspective. *Chem. Phys. Lett.* **1997**, *281*, 130−134.

(34) East, A. L. L.; Allen, W. D. The heat of formation of NCO. *J. Chem. Phys.* **1993**, *99*, 4638−4650.

(35) Simmonett, A. C.; Schaefer, H. F.; Allen, W. D. Enthalpy of formation and anharmonic force field of diacetylene. *J. Chem. Phys.* **2009**, *130*, 044301.

(36) Feller, D. The use of systematic sequences of wave functions for estimating the complete basis set, full configuration interaction limit in water. *J. Chem. Phys.* **1993**, *98*, 7059−7071.

(37) Helgaker, T.; Klopper, W.; Koch, H.; Noga, J. Basis-set convergence of correlated calculations on water. *J. Chem. Phys.* **1997**, *106*, 9639−9646.

(38) Bomble, Y. J.; Stanton, J. F.; Kállay, M.; Gauss, J. Coupled-cluster methods including noniterative corrections for quadruple excitations. *J. Chem. Phys.* **2005**, *123*, 054101.

(39) Handy, N. C.; Yamaguchi, Y.; Schaefer, H. F. The diagonal correction to the Born−Oppenheimer approximation: Its effect on the singlet−triplet splitting of $CH_2$ and other molecular effects. *J. Chem. Phys.* **1986**, *84*, 4481−4484.

(40) Gauss, J.; Tajti, A.; Kállay, M.; Stanton, J. F.; Szalay, P. G. Analytic calculation of the diagonal Born-Oppenheimer correction

within configuration-interaction and coupled-cluster theory. *J. Chem. Phys.* **2006**, *125*, 144111.
(41) Tajti, A.; Szalay, P. G.; Gauss, J. Perturbative treatment of the electron-correlation contribution to the diagonal Born-Oppenheimer correction. *J. Chem. Phys.* **2007**, *127*, 014102.
(42) Szalay, P. G.; Gauss, J.; Stanton, J. F. Analytic UHF-CCSD(T) second derivatives: implementation and application to the calculation of the vibration-rotation interaction constants of NCO and NCS. *Theor. Chim. Acta.* **1998**, *100*, 5−11.
(43) Harding, M. E.; Metzroth, T.; Gauss, J.; Auer, A. A. Parallel Calculation of CCSD and CCSD(T) Analytic First and Second Derivatives. *J. Chem. Theory Comput.* **2008**, *4*, 64−74.
(44) Nielsen, H. The Vibration-Rotation Energies of Molecules. *Rev. Mod. Phys.* **1951**, *23*, 90−136.
(45) CFOUR, a quantum chemical program package written by Stanton, , J. F.; Gauss, , J.; Watts, , J. D.; Szalay, , P. G.; Bartlett, , R. J. with contributions from Auer, , A. A.; Bernholdt, , D. E.; Christiansen, , O.; Harding, , M. E.; Heckert, , M., ; et al. For the currentversion see, http://www.cfour.de.
(46) Werner, H.-J. et al. MOLPRO, version 2010.1, a package of ab initio programs. 2010; see http://www.molpro.net.
(47) Kállay, M.; Surján, P. R. Higher excitations in coupled-cluster theory. *J. Chem. Phys.* **2001**, *115*, 2945.
(48) Kállay, M.; Gauss, J. Approximate treatment of higher excitations in coupled-cluster theory. *J. Chem. Phys.* **2005**, *123*, 214105.
(49) Wiberg, K. B. Application of the pople-santry-segal CNDO method to the cyclopropylcarbinyl and cyclobutyl cation and to bicyclobutane. *Tetrahedron* **1968**, *24*, 1083−1096.
(50) Sherrill, C. D.; Van Huis, T. J.; Yamaguchi, Y.; Schaefer, H. F. Full configuration interaction benchmarks for the states of methylene. *J. Mol. Struct.* **1997**, *400*, 139−156.
(51) Walsh, A. D. 466. The electronic orbitals, shapes, and spectra of polyatomic molecules. Part I. $AH_2$ molecules. *J. Chem. Soc.* **1953**, 2260−2266.